

Ce-catalyzed oxidation of Ta(110)

C. Gu, D. W. Lynch, A. B. Yang, and C. G. Olson

Department of Physics and Ames Laboratory, Iowa State University, Ames, Iowa 50011

(Received 18 October 1989; revised manuscript received 8 March 1990)

Photoemission spectroscopy was used to investigate the initial oxidation of the Ce/Ta(110) interface at room temperature. The oxidation of Ta(110) is dramatically enhanced by a thin Ce overlayer. A Ta suboxide TaO_χ ($0.5 \leq \chi \leq 1$) is formed first in the interface, followed by the rapid formation of Ta_2O_5 upon further oxygen exposure. A weak interface reaction exists in Ce/Ta(110), but is excluded as the main cause of the catalytic oxidation. An earlier suggestion is reconfirmed that the Ce layer converts O_2 to oxygen ions and thus promotes the oxidation of the substrate.

I. INTRODUCTION

Since the discovery of the catalytic effect of Ce on the oxidation of Nb,¹ a series of studies²⁻⁵ on surface oxidation have been carried out in light of the new finding. X-ray photoemission spectroscopy (XPS) measurements of Nb 3*d* levels revealed that at room temperature, significant amounts of bulk Nb_2O_5 are formed at low oxygen exposure, promoted by a thin Ce overlayer.^{1,2} High oxygen-ion mobility in the Ce overlayer is considered to be the cause of the fast oxygen diffusion. Some other rare-earth metals, such as Pr and Tb, have similar but less impressive capabilities for enhancing the oxidation of Nb.³ Ce also enhances the oxidation of Si.⁴ However, unlike the Ce/Nb interface which was claimed to be non-reactive, Ce itself reacts strongly with Si.^{4,6}

Although NbO and various other Nb oxides form in the oxidation of pure Nb, only Nb_2O_5 was observed in the growth of a Ce/Nb oxide film. Based on this observation, it was proposed⁵ that during the oxidation of pure Nb(110), a Nb suboxide layer (NbO) formed on the surface is a barrier to further oxygen penetration due to higher embedding energy for the oxygen atom. Thus the rapid oxidation of Ce/Nb may be a direct consequence of the lack of a NbO barrier. However, XPS studies of the Nb 3*d* core levels are not very surface sensitive due to the large electron kinetic energy involved (10^3 eV).¹ To study details of the initial stages in the catalytic oxidation, we choose Ta(110) as the substrate, because the Ta 4*f* core levels are very sharp and can be measured by surface-sensitive soft-x-ray photoemission spectroscopy with synchrotron radiation sources. The use of a single crystal as the substrate eliminates possible grain-boundary effects⁷ in the oxidation. More important, analyses of the Ta(110) surface core-level shifts allow us to probe the Ce/Ta interface reaction. As compared with the XPS study of Ce/Nb, the better surface sensitivity and resolution in this experiment make it much easier to study the early stages of the catalytic oxidation, which are certainly important for understanding the kinetics of the catalytic action and the general surface oxidation itself.

In this experiment, we evaporated 4.5 Å of Ce on Ta(110). Changes in the Ta 4*f* core levels are evident

upon Ce adsorption. Curve fitting is used to reveal changes of the surface components. The Ce/Ta interface reaction is discussed in terms of the Ta surface core-level shifts. After exposing the Ce/Ta(110) surface to 1×10^{-8} Torr O_2 at room temperature, it is seen that the Ce overlayer significantly promotes the oxidation of Ta(110). The growth pattern of the Ta oxides is totally different from that without the Ce catalyst. Two Ta oxide states, TaO_χ ($0.5 \leq \chi \leq 1$) and Ta_2O_5 , dominate the initial oxidation. A thin TaO_χ layer is formed first, but is further oxidized to Ta_2O_5 quickly upon more oxidation. The Ce overlayer was studied by measurements of the valence spectra and the Ce 4*d* absorption spectra. Observation of the Ce oxide states reconfirms earlier suggestions¹⁻³ that changes between the two Ce valence states (Ce^{3+} and Ce^{4+}) promote the oxygen-ion diffusion from surface to substrate.

II. EXPERIMENTAL

The photoemission experiments were performed at the Iowa State University–Montana State University ERG-Seya beamline⁸ at the Synchrotron Radiation Center (Stoughton, WI), University of Wisconsin–Madison. The combined ERG-Seya monochromators provide photon energies from 5 to 1200 eV. The Ta(110) crystal, $2 \times 2 \times 1$ mm³, was prepared by the Ames Laboratory. The Ta crystal was cleaned by annealing *in situ* at an extremely high temperature ($\sim 2600^\circ\text{C}$) to expel oxygen from the bulk Ta. High-voltage electron-beam bombardment was employed to heat the sample efficiently. The temperature was monitored by an optical pyrometer. After 4 h of annealing, the Ta(110) was clean, as checked by the valence spectrum (Fig. 1, curve A) and the Ta 4*f* core-level spectrum (Fig. 2, curve A). The line shape of the Ta 4*f* levels is very sensitive to the surface condition. Oxygen contamination will cause the surface components to shift to higher binding energies. The (110) low-energy electron-diffraction (LEED) pattern was checked in another chamber after similar cleaning procedures. Before each experiment, the sample was flashed to high temperature to remove any residual contamination from the surface. The base pressure was about 1×10^{-10} Torr. The pressure only rose to 3×10^{-10} Torr during the high-

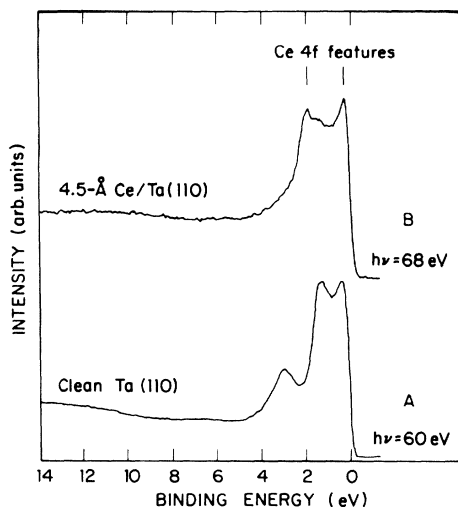


FIG. 1. Valence-band spectra of clean Ta(110) and Ce/Ta(110). In *B* two Ce 4*f*-related features are identified at 2.0 and 0.2 eV.

temperature flashing. A piece of high-purity Ce metal was also provided by the Ames Laboratory. The Ce metal was melted and degassed thoroughly. After 8 h of degassing, 4.5 Å of Ce was evaporated onto the Ta(110) surface. Figure 1, curve *B* shows the valence-band spectrum taken after the evaporation with $h\nu = 68$ eV. Two Ce 4*f*-related features^{9,10} can be seen at 2 eV and near the Fermi level (0.2 eV). There is no sign of oxygen contamination around 6-eV binding energy.

III. RESULTS AND DISCUSSION

A. Ta surface core-level shifts: The Ce/Ta interface reaction

Figure 3 shows the detailed Ta 4*f*_{7/2} levels before and after Ce adsorption. The surface core-level shifts for various Ta surfaces are well known.¹¹ For Ta(110), only the first surface layer contributes significant core-level shifts.¹¹ Therefore the Ta 4*f*_{7/2} spectra can be fitted by one surface level (*S*) in addition to the bulk level (*B*). Each component has the Doniach-Šunjić (DS) line shape¹² convolved with a Gaussian broadening function. To reduce the number of independent parameters, we may assume the hole lifetime ($1/\gamma$) and the singularity index (α) in the surface component are the same as in the bulk component.¹³ However, as noted in Ref. 13, the Gaussian widths (Γ^G) may be different. The Gaussian broadening represents contributions from the instrumental resolution function, phonon excitation, and other possible sources of inhomogeneous broadening. It was found that the surface components in Ta(111) have broader Gaussian features than the bulk components.¹³ The differences in the Gaussian widths were tentatively attributed to unresolved surface crystal-field splitting.¹³

The best least-squares fit for Ta 4*f*_{7/2} of clean Ta(110) is obtained by adjusting the parameters to the values tabulated in Table I. The background is approximated by a straight line. For comparison, some parameters given by

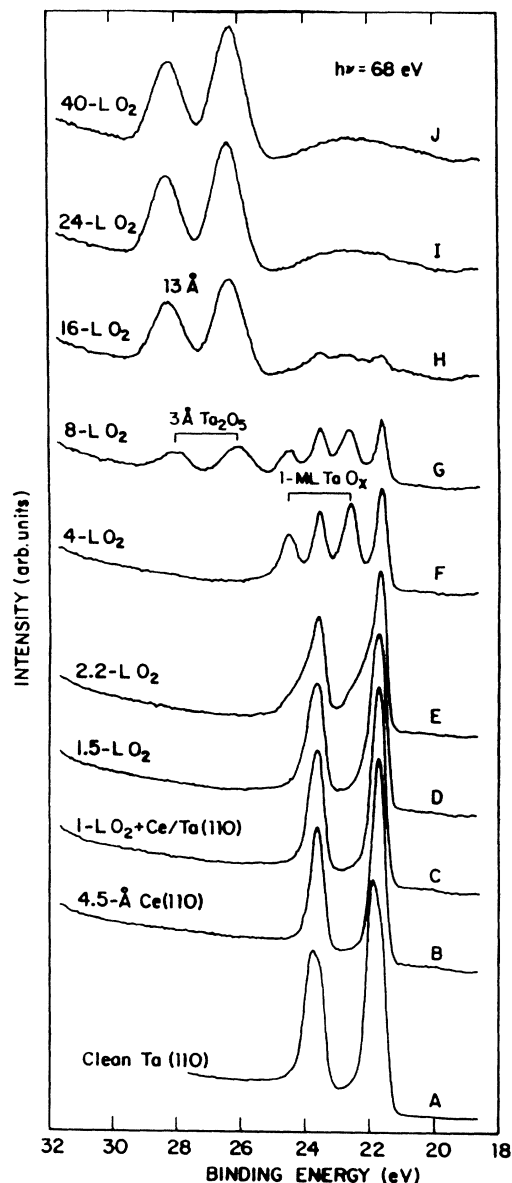


FIG. 2. Ta 4*f* spectra. *A* and *B* are for clean Ta(110) and Ce/Ta(110), respectively. *C*-*J* were taken after Ce/Ta(110) was exposed to various amounts of O₂ at 1×10^{-8} Torr.

other work are also listed. Values of the Lorentzian width Γ ($=2\gamma$), the singularity index α , and the surface 4*f* level shift Δ_{surf} are generally in agreement with other work. The instrumental resolution in the experiment is 265 meV. The phonon broadening in Ta can be as much as 167 meV, as estimated by Flynn.¹⁴ Thus the combined Gaussian width should be about 313 meV, very close to the bulk Gaussian width (Γ_{bulk}^G) obtained in our fit. The Gaussian width in the surface component Γ_{surf}^G is larger than Γ_{bulk}^G . As in Ta(111), unresolved surface crystal-field splitting may be considered as the source of the extra broadening.

After 4.5 Å of Ce was evaporated on the Ta(110) surface, the Ta 4*f*_{7/2} surface component shifts toward the

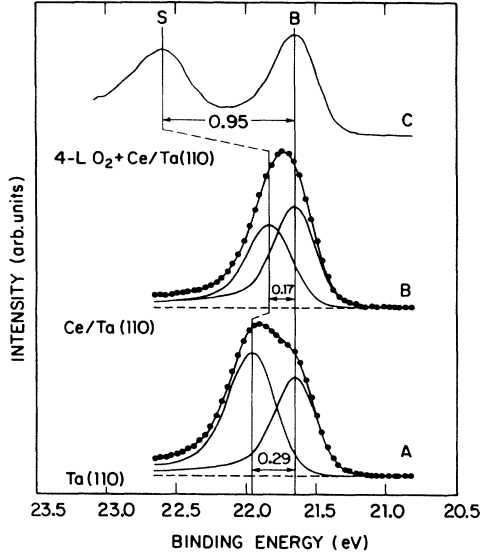


FIG. 3. Ta $4f_{7/2}$ spectra in which the surface and bulk components are separated by either curve fitting *A*, *B*, or oxidation *C*.

bulk core level by 0.12 eV, making the overall line shape much sharper (Fig. 3, curve *B*). The same values of $\Gamma(2\gamma)$, α , and Γ_{bulk}^G have been used in the fitting. The Gaussian width for the surface component is found to be closer to the bulk value, indicating that the surface crystal-field splitting is weaker for the Ta/Ce interface than the Ta/vacuum interface.

The smaller surface core-level shift in Ce/Ta(110) can be the result of two effects: (1) electron donation from Ce to the Ta valence band and (2) the rebroadening of the Ta surface valence band due to bonding between Ce and Ta. The influence of a donor adsorbate (Cs) on Ta(100) and W(100) was reported before.¹⁵ In our case, Ce may also be considered an electron donor since Ce has a lower electronegativity (1.03) than Ta (1.33).¹⁶ A small amount of electron charge may be transferred from Ce to Ta. Therefore the Ta surface core level should shift to lower binding energy due to increased electron screening. To understand the second effect, we need to consider the origin of the surface core-level shifts for transition metals like Ta.¹⁷ The reduced coordination number of atoms on metal surfaces usually results in a narrowing of the valence band. The major effect of the band narrowing is to raise (or lower) the Fermi level of the surface band, de-

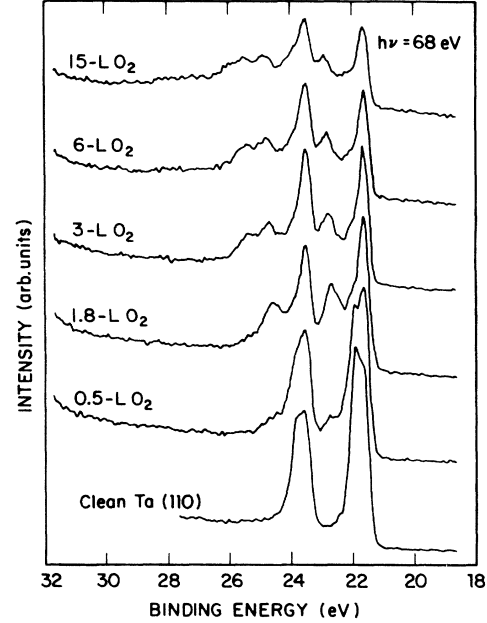


FIG. 4. Ta $4f$ spectra after Ta(110) was exposed to 1×10^{-8} Torr O_2 for various periods.

pending on whether the d band is less (or more) than half-filled. To restore equilibrium and bring the Fermi level back to the bulk level, a small amount of charge must transfer out of (or into) the surface bands. The small charge change in the surface thus lowers (or raises) the energies of all electrons in the surface. For Ta, the d band is less than half-filled, so the surface core levels shift to higher binding energies. The Ce overlayer makes the Ta surface more bulklike. Ce—Ta bonding rebroadens the narrowed Ta surface valence band. The resulting Ta surface line-shape parameters are closer to the bulk. Since the Ta surface layer still exhibits a shift of +0.17 eV, the Ce—Ta bond is weaker than the Ta—Ta bond. Thus a reaction between Ta and the physisorbed Ce exists but it tends to be small. We further believe that at room temperature there is no interdiffusion between Ce and Ta, as illustrated later in the oxidation of Ce/Ta.

B. Oxidation of Ce/Ta(110): The catalytic effect

For purposes of comparison, the oxidation of Ta(110) itself was investigated. Figure 4 shows a sequence of Ta $4f$ spectra after clean Ta(110) was exposed to oxygen

TABLE I. Summary of Ta $4f_{7/2}$ line-shape parameters.

	Present		Others
	Ta(110)	Ce/Ta(110)	
Δ_{surf} (eV)	0.29	0.17	0.28 [Ta(110), Ref. 11]
$\Gamma(2\gamma)$ (eV)	0.05	0.05	0.04 [Ta(111), Ref. 13]
α	0.12	0.12	0.15 [Ta(111), Ref. 13]
Γ_{bulk}^G (eV)	0.31	0.31	
Γ_{surf}^G (eV)	0.35	0.33	

at 1×10^{-8} Torr. (We want to point out that in this work oxidations were performed cumulatively and the O_2 exposure values shown are the total amounts. Spectra in Figs. 2, 4, 5, and 6 are normalized by the photoyield current from a monitoring mesh which is approximately proportional to the photon flux.) We note that a small amount of O_2 exposure (0.5 L) can induce noticeable chemical shifts. After a total of 15 L O_2 exposure, some Ta suboxides with chemical shifts of less than 3 eV are formed in the surface. [1 langmuir (L) $\equiv 10^{-6}$ Torr sec.]

Figure 2 shows the Ta 4f spectra for the oxidation of Ce/Ta(110) at the same O_2 pressure. From spectra C and D one can see virtually no Ta oxidation during the initial exposures (≤ 1.5 L), since the Ce layer on top was oxidized first. In fact, assuming that the Ce atoms stay on top of Ta uniformly and are all oxidized to Ce_2O_3 , one may estimate that the Ta under 4.5 Å Ce would not be reached by oxygen until 2.7 L O_2 exposure. In our experiment, the Ta oxidation "threshold" is near 2.2 L O_2 exposure (spectrum E), which is a good indication that Ce covered the Ta surface quite uniformly and no significant Ce/Ta mixture or interdiffusion occurs. After a total of 4 L O_2 exposure, a pair of well-defined shifted peaks appears at binding energies 0.95 eV higher than the bulk levels, indicating the formation of a Ta suboxide, which we call TaO_x . More oxygen exposures (from G to J) result in the fast growth of Ta_2O_5 , which is represented by a large chemical shift ($\sim +5$ eV) in the core levels. The very broad feature near 22 eV in G–J is the $O 2s$ level. After 16 L O_2 exposure, 13 Å of Ta_2O_5 have grown.¹⁸ In I after 24 L O_2 exposure the thickness of Ta_2O_5 is already beyond the probing depth. Comparing with the oxidation of pure Ta(110) (Fig. 4), we conclude that the oxidation of Ta is dramatically enhanced by the Ce on top.

The formation of the Ta suboxide TaO_x surprised us since no Nb suboxide was observed in the Ce/Nb oxidation. It is also very interesting to note that the well-defined TaO_x is the only suboxide in the oxidation. If we compare the $4f_{7/2}$ components after 4 L O_2 exposure with the fitted Ta $4f_{7/2}$ level in Ce/Ta(110) (Fig. 3, curves C and B), it is obvious that almost the entire first Ta layer becomes TaO_x , as the whole surface component shifts from the bulk level by +0.95 eV.

Meanwhile, the identification of TaO_x proves to be less straightforward. Oxidation of Ta under different conditions (usually at elevated temperatures) has been investi-

gated for many years.^{20–27} A few types of Ta suboxide, TaO_x (Ta_6O), TaO_y (Ta_2O), TaO_z (Ta_2O), TaO, and TaO_2 , were detected by x-ray-diffraction and weight-gain measurements.²⁰ Unfortunately, almost all of them were not in pure form, thus the assigned formulae are stoichiometrically approximate. In the photoemission spectroscopy area, interpretations of chemical shifts in Ta suboxides are correspondingly controversial^{21–24} (see Table II), since the suboxides cannot be prepared well enough. Sanz and Hofmann²¹ oxidized Ta at room temperature and analyzed the core-level spectra (obtained by XPS) in an analogy with the oxidation of Nb. Three chemical shifts were identified in their deconvolution of the oxide spectra. TaO and TaO_2 were assigned to the chemical shifts of 2.0 and 3.9 eV, respectively. However, with better resolution and higher surface sensitivity, our Ta oxidation spectra (Fig. 4) clearly reveal the existence of two chemical shifts of less than 2.5 eV. We also note that these shifted peaks may move to higher binding energies upon further oxidation. Chemical shifts ranging from 0.5 to 2.4 eV were reported in the initial oxidation of Ta(111) at room temperature.²⁵ A similar experiment was done on Ta(100), and a shift of ~ 1.5 eV was thought to be related to TaO.²² LEED studies^{26,27} on the oxidation of Ta surfaces did show some ordered structures, but only after annealing. It is generally accepted that at room temperature Ta surfaces oxidize in an almost amorphous fashion. So the deconvolution of Ta oxide spectra shown in Ref. 21 can only be considered as a rough evaluation of the Ta oxidation states. Photoemission studies on Ta oxidation at higher temperatures were carried out by Legma *et al.*²³ and Himpfel *et al.*²⁴ At elevated temperatures, oxygen diffusion and oxidation are much faster. The oxide products are quite different under varied conditions. Reference 23 identified the oxidation products after comparing them with Nb oxides. Reference 24 is a parallel oxidation study of W and Ta. One of the key conclusions in Ref. 24 is that there is a significant discontinuity of binding energy (2–3 eV) between metallic and dielectric (insulating) screening. Consequently, chemical shifts of less than 2 eV were assigned to Ta oxide states relatively higher than in other studies, and the 2.05-eV shift was referred to as a formal metallic Ta^{5+} state, which is unknown so far.

The oxidation of Ce/Ta(110) is unlike that of Ta reported at any temperature region. Therefore as we com-

TABLE II. Chemical shifts of Ta 4f levels (in eV relative to the bulk) for Ta surface oxides. The notion (metallic) is used only for the convenience to accommodate the results of Ref. 24. Some values shown are the averages of all data given in the literature. The TaO_x with a 0.95-eV shift is close to Ta^{1+} and Ta^{2+} . See text for details.

Ta Oxides	(Metallic)					Insulating
	1+	2+	3+	4+	5+	5+
Ref. 21		2.0		3.9		5.0
Ref. 22		1.5				
Ref. 23	0.5	1.3	> 1.8			5.2
Ref. 24	0.48		1.22		2.05	5.2
Ce/Ta(110)+ O_2		0.95				5.1

pare TaO_x to the results shown in Table II, it is not justified to favor or disfavor any of these studies based on oxidation conditions. Considering all earlier work and data in Table II, we feel it is appropriate to assign Ta^{2+} (TaO) as the upper limit and Ta^{1+} (Ta_2O) as the lower limit for the oxidation state of TaO_x ($0.5 \leq \chi \leq 1$). Since the TaO_x is actually very thin (1 ML), this kind of estimate seems reasonable.

In Fig. 2, curves *G* and *H*, the TaO_x and Ta signals become smaller, and Ta_2O_5 shows up during oxidation. It was mentioned earlier that all spectra in Fig. 2 are normalized and the thicknesses of Ta_2O_5 were estimated in Ref. 18. Some possibilities regarding the growth of Ta_2O_5 and TaO_x can be evaluated by studying Fig. 2, curves *F*–*H*. Since there is not much Ce/Ta mixture, the oxidation can be assumed to be relatively homogeneous. Thus it is natural to believe the interface layer TaO_x should be first oxidized to Ta_2O_5 in Fig. 2, curve *G*. On the other hand, because the relative intensity of TaO_x compared with that of Ta does not change much, it has to be recognized that some new TaO_x is formed at the same time. (The electron mean free path in Ta_2O_5 is much larger than that in Ta or TaO_x , the transformation of TaO_x to Ta_2O_5 in Fig. 2, curve *G* should not reduce the Ta signals.) From Fig. 2, curves *G* and *H*, it may be estimated that the average amount of TaO_x never exceeds the initial 1 ML at any time.

To study the role of the Ce layer in the oxidation, we measured the valence spectra (Fig. 5) and constant final-state (CFS) spectra in the region of Ce $4d$ absorption edges (Fig. 6). The valence spectrum of clean Ce/Ta(110) mainly exhibits Ce features due to the uniform Ce coverage and the small electron escape depth in the range of kinetic energies involved (see Fig. 1 for a better view). As mentioned earlier, there are two Ce $4f$ -related

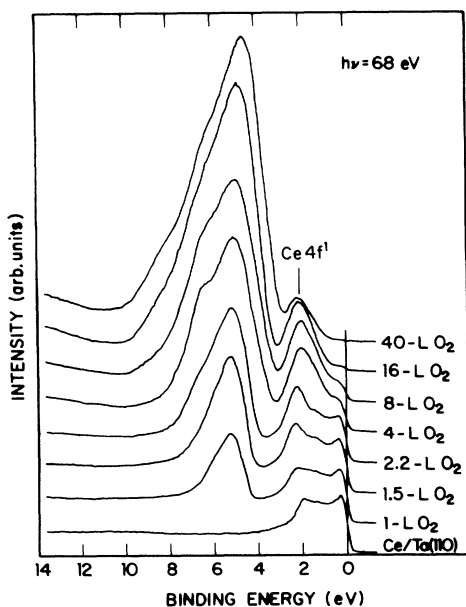


FIG. 5. Valence-band spectra of Ce/Ta(110) as a function of O_2 exposure.

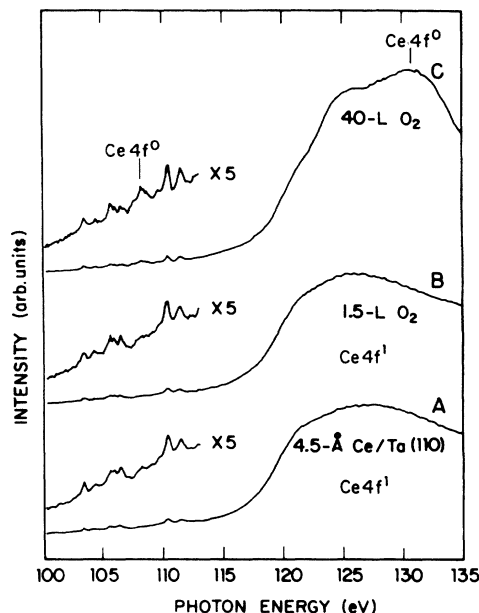


FIG. 6. CFS spectra in the region of Ce $4d$ absorption edges.

features^{9,10} located at 2.0 and 0.2 eV, respectively. The first one is regarded as the (shifted) localized $4f^1$ core level. The second feature near E_f (not well resolved) is due to the hybridization between $4f$ and the valence band. Upon oxidation, broad $\text{O}2p$ -related structures emerge around 5–6 eV, while the density of states near E_f decreases. The Ce $4f$ level at 2.0 eV shifts to about 2.4 eV after oxidation, consistent with other work.²⁸ The intensity ratio between this Ce $4f$ level and the peak near E_f increases after 1.5–4 L O_2 exposure. This may be the result of the decreased hybridization, since the valence band near E_f disappears under oxidation. After 40 L O_2 , the density of states close to the Fermi level ceases to exist, corresponding to the formation of an insulator at the surface. At the same time, the intensity of the Ce $4f$ level drops, indicating the transformation of some Ce_2O_3 ($\text{Ce}^{3+}, 4f^1$) to CeO_2 ($\text{Ce}^{4+}, 4f^0$).

The formation of Ce^{4+} is also demonstrated by the CFS spectra taken in the region of the Ce $4d^{10}4f^n \rightarrow 4d^94f^{n+1}$ absorption edges (Fig. 6). The absorption spectra consist of two parts: a fine-structure part from 100 to 113 eV (enlarged), and a strong wide band in the region of 120–135 eV. The absorption structures are very sensitive to the occupancy of the $4f$ level.^{10,29} The spectra of pure Ce and Ce_2O_3 are similar (Fig. 6, curves *A* and *B*) since the Ce is trivalent ($4f^1$) in both materials. However, as Ce becomes nominally tetravalent ($4f^0$) in CeO_2 , the spectrum looks very different, resembling that of La^{3+} , but shifted in energy.²⁹ In Fig. 6, curve *C*, after 40 L O_2 exposure, a mixture of Ce^{3+} and Ce^{4+} spectra is found. A new peak at 108 eV in the fine structure and another new broad feature around 130 eV are characteristic of the tetravalent Ce. From the relative intensities of the Ce^{3+} and Ce^{4+} features in the fine structure, we learn that a significant

portion of Ce_2O_3 still remains on the surface. Actually, in the valence spectra, the intensity of the Ce 4*f* level after 40 L O_2 drops about 40%, so there is 60% of Ce_2O_3 on the surface. The unusually slow oxidation saturation of the very thin Ce layer (4.5 Å) is directly related to its role in the oxidation of the Ta substrate. In fact, it was proposed that the catalytic oxidation is connected to the valence changes between 3+ and 4+ in the oxidized Ce.¹⁻³ The Ce_2O_3 layer on the surface reacts with adsorbed oxygen atoms to form CeO_2 . However, CeO_2 is an oxygen-ion conductor with a high oxygen-ion mobility.¹ The CeO_2 may easily lose oxygen ions to the substrate and change back to Ce_2O_3 . Therefore, the Ce oxide layer converts adsorbed O_2 to oxygen ions which may diffuse into the substrate below. As long as the oxygen-ion diffusion into Ta is not slow compared with the oxygen dose (1×10^{-8} Torr), the Ce overlayer should appear to be in the lower-oxidation state as Ce_2O_3 . In this experiment, the Ce layer remains as Ce_2O_3 until the oxidation of Ta begins to slow down after ~ 40 L O_2 exposure. Therefore we believe the earlier suggestion on the role of Ce is correct.

The weak Ce/Ta interface reaction mentioned earlier might initially help the oxygen-ion transfer from Ce to Ta. But after Ta_2O_5 forms beneath Ce, the interface reaction is totally lost, therefore further fast oxidation could not be explained by this mechanism.

IV. SUMMARY

From the experimental results discussed, the conclusions are summarized as follows.

Oxidation of Ta(110) is dramatically enhanced by a Ce overlayer at room temperature. One monolayer of Ta is oxidized to TaO_χ ($0.5 \leq \chi \leq 1$) first, in contrast with ear-

lier observations on the Ce/Nb oxidation. The catalytic oxidation of Ta does not slow down after the formation of TaO_χ . Bulk Ta_2O_5 forms after only 8 L O_2 exposure.

From the analyses of the Ta surface 4*f* core levels, we conclude the Ce overlayer only weakly reacts with the Ta substrate by a weak bonding to Ta and/or a small amount of electron donation to Ta. No Ce/Ta interdiffusion or mixture was found. The weak Ce/Ta reaction is not considered to be the main cause of the catalytic reaction.

We have confirmed that the Ce oxidation state changes between CeO_2 and Ce_2O_3 , providing oxygen ions (instead of O_2 molecules), thus promoting the oxidation of the metal substrate.

After this paper was submitted, a paper by Braaten *et al.*³⁰ appeared. Polycrystalline Ta was used in their experiments. The same conclusions were reached on the existence of the catalytic effect of Ce on Ta oxidation and the corresponding mechanism. Our work differs in the findings of the weak Ce/Ta(110) interface reaction and the clear formation of TaO_χ in the oxidation of Ce/Ta(110). These detailed insights might be attributed to the use of single crystal Ta as the substrate.

ACKNOWLEDGMENTS

We wish to acknowledge the receipt of pure Ce from B. J. Beaudry of the Ames Laboratory and the Ta(110) crystal from T. Lograsso of the Ames Laboratory, and help from the staff of the Synchrotron Radiation Center. The Ames Laboratory is operated for the U.S. Department of Energy by Iowa State University under Contract No. W-7405-ENG-82. The Synchrotron Radiation Center is operated by the University of Wisconsin under National Science Foundation Contract No. DMR-86-01349.

¹E.-E. Latta and M. Ronay, *Phys. Rev. Lett.* **53**, 948 (1984).

²M. Ronay and E.-E. Latta, *Phys. Rev. B* **32**, 5375 (1985).

³E.-E. Latta and Maria Ronay, *J. Vac. Sci. Technol. A* **4**, 1626 (1986).

⁴F. U. Hillebrecht, M. Ronay, D. Rieger, and F. J. Himpsel, *Phys. Rev. B* **34**, 5377 (1986).

⁵M. Ronay and P. Nordlander, *Phys. Rev. B* **35**, 9403 (1987).

⁶M. Grioni, J. Joyce, S. A. Chambers, D. G. O'Neill, M. del Giudice, and J. H. Weaver, *Phys. Rev. Lett.* **53**, 2331 (1984).

⁷S. Lugomer, M. Kerenovic, M. Stipanovic, and S. Lekic, *Vacuum* **38**, 15 (1988).

⁸C. G. Olson, *Nucl. Instrum. Methods Phys. Res. Sect.* **266**, 205 (1988).

⁹D. Wieliczka, J. H. Weaver, D. W. Lynch, and C. G. Olson, *Phys. Rev. B* **26**, 7056 (1982).

¹⁰D. W. Lynch and J. H. Weaver, in *Handbook on the Physics and Chemistry of Rare Earths*, Vol. 10, edited by K. A. Gschneidner, Jr., L. Eyring, and S. Hüfner (North-Holland, New York, 1987), Chap. 66 and references therein.

¹¹D. Spanjaard, C. Guillot, M.-C. Desjonqueres, G. Treglia, and J. Lecante, *Surf. Sci. Rep.* **5**, 1 (1985).

¹²S. Doniach and M. Šunjić, *J. Phys. C* **3**, 285 (1970).

¹³G. K. Wertheim, P. H. Citrin, and J. F. van der Veen, *Phys.*

Rev. B **30**, 4343 (1984).

¹⁴C. P. Flynn, *Phys. Rev. Lett.* **37**, 1445 (1976).

¹⁵P. Soukiassian, R. Riwan, J. Cousty, J. Lecante, and C. Guillot, *Surf. Sci.* **152/153**, 290 (1985).

¹⁶R. Rich, *Periodic Correlations* (Benjamin, New York, 1965), p. 50.

¹⁷P. H. Citrin and G. K. Wertheim, *Phys. Rev. B* **27**, 3176 (1983).

¹⁸Suppose Ta_2O_5 is on top of TaO_χ and Ta, the thicknesses of Ta_2O_5 shown in Fig. 2 were estimated by $t_{\text{ox}} = \lambda_{\text{ox}} \cos \theta \ln [I_t / (I_t - I_{\text{ox}})]$, where I_t and I_{ox} refer to the total core-level emission and the emission from Ta_2O_5 , respectively. λ_{ox} ($= 8.7$ Å) is the electron mean free path in Ta_2O_5 calculated with the equation provided in Ref. 19. We use $\theta = 42.3^\circ$ [the acceptance angle of the cylindrical mirror analyzer (CMA)], although the sample surface was tilted. The possible deviation caused by this approximation was estimated to be surprisingly small (a few percent).

¹⁹M. P. Seah and W. A. Dench, *Surf. Interface Anal.* **1**, 2 (1979).

²⁰*Gmelins Handbuch der Anorganischen Chemie*, System No. 50, Tantal B-Lieferung 1 (Verlag Chemie, Weinheim, 1970), p. 23 and references therein.

²¹J. M. Sanz and S. Hofmann, *J. Less-Common Met.* **92**, 137

- (1983).
- ²²C. Guillot, P. Roubin, J. Lecante, M. C. Desjonqueres, G. Treglia, D. Spanjaard, and Y. Jugnet, *Phys. Rev. B* **30**, 5487 (1984).
- ²³B. Legma, D. Simon, P. Baillif, and J. Bardolle, *J. Less-Common Met.* **95**, 37 (1983).
- ²⁴F. J. Himpsel, J. F. Morar, F. R. McFeely, R. A. Pollak, and G. Hollinger, *Phys. Rev. B* **30**, 7236 (1984).
- ²⁵J. F. van der Veen, F. J. Himpsel, and D. E. Eastman, *Phys. Rev. B* **25**, 7388 (1982).
- ²⁶J. E. Boggio and H. E. Farnsworth, *Surf. Sci.* **3**, 62 (1964).
- ²⁷M. A. Chesters, B. J. Hopkins, and M. R. Leggett, *Surf. Sci.* **43**, 1 (1974).
- ²⁸A. Platau and S.-E. Karlsson, *Phys. Rev. B* **18**, 3820 (1978).
- ²⁹T. M. Zimkina and I. I. Lyakhovskaya, *Fiz. Tverd. Tela (Leningrad)* **18**, 1143 (1976) [*Sov. Phys.—Solid State* **18**, 655 (1976)].
- ³⁰N. A. Braaten, J. K. Grepstad, and S. Raaen, *Surf. Sci.* **222**, 499 (1989).